ACS OMEGA

http://pubs.acs.org/journal/acsodf

Article

Regioselective Synthesis of 2-Aryl-5-cyano-1-(2-hydroxyaryl)-1*H*-imidazole-4-carboxamides Self-Assisted by a 2-Hydroxyaryl Group

Fábio Pedroso de Lima,[§] Emilio Lence,[§] Pilar Suárez de Cepeda, Carla Correia, M. Alice Carvalho, Concepción González-Bello,* and M. Fernanda Proença*

Cite This: *ACS Omega* 2022, 7, 23289−23301

Read Online

ACCESS | Metrics & More | Article Recommendations | Supporting Information

ABSTRACT: The reactivity of the diaminomaleonitrile-based imines containing hydroxyphenyl substituents with diverse aromatic aldehydes has been explored for the synthesis of novel highly substituted nitrogen heterocycles, which are considered privileged scaffolds in drug discovery. We report here a simple and efficient method for the regiocontrolled synthesis of a variety of 2-aryl-5-cyano-1-(2-hydroxyaryl)-1*H*-imidazole-4-carboxamides from 2-hydroxybenzylidene imines and aromatic aldehydes. Computational studies on the reaction path revealed that the regioselectivity of the reaction toward the formation of imidazole derivatives instead of 1,2-dihydropyrazines, most likely *via* a diaza-Cope rearrangement, is driven by the 2-hydroxyaryl group in the scaffold. The latter group promotes the intramolecular abstraction and protonation process in the cycloadduct intermediate, triggering the evolution of the reaction toward the formation of imidazole derivatives.

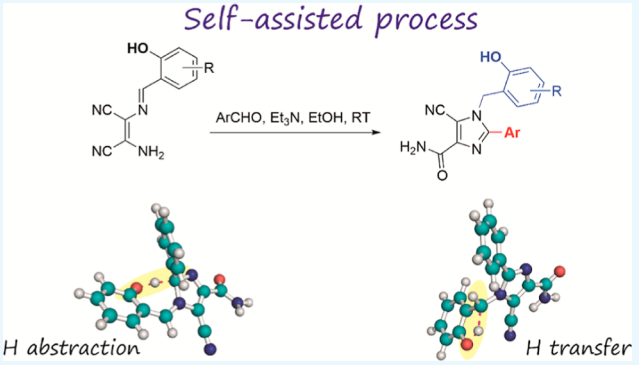

INTRODUCTION

Diaminomaleonitrile (DAMN) is a versatile building block in organic synthesis, extensively used as a precursor in the preparation of a large variety of nitrogen heterocycles,[1] including pyrimidines,[2] pyrazines,[3,4] purines,[5−7] adenines,[8] imidazoles,[9,10] and pyrroles,[11,12] among others. The synthetic scheme to achieve these compounds usually involves the modification of one of the amino groups in DAMN by the reaction with aldehydes, orthoformate, acid chlorides, acid anhydrides, or isocyanates, followed by an intramolecular condensation reaction.[1] In other cases, before the condensation, the modification of the remaining free amino group is performed to expand the chemical space, as well as to get access to more complex heterocycles.

Among the DAMN-based intermediates employed in those approaches, benzylidene imines **1** proved to be versatile and readily accessible intermediates for the synthesis of highly substituted imidazoles and pyrazines (Figure 1).[13] These nitrogen heterocycles are considered privileged scaffolds in drug discovery and are the pharmacophore in numerous successful drugs in clinical use, such as eprosartan (antihypertensive agent), metronidazole (antibiotic and antiparasitic agent), and gilteritinib (anticancer agent), among others.[14−23]

Examples of synthetic approaches employing benzylidene imines **1** are disclosed in Scheme 1. The treatment of **1** with either MnO_2,[9] nicotinamide/*N*-chlorosuccinimide (NCS),[24] or copper-modified manganese oxide-based octahedral molecular sieves (CuO_x/OMS-2)[10] afforded 2-aryl-4,5-dicyanoimidazoles **2** in yields ranging from 48 to 93%. The reaction is suitable for a large variety of substituents (electron-donating and electron-withdrawing groups), as well as positions (*ortho*, *meta*, and *para*) in the ring. On the other hand, substituted pyrazine carboxamides **5** could be synthesized in two steps from dibenzylidene imines **3**, which are obtained from the treatment of **1** with benzaldehydes in the presence of triethylamine in 68−73% yields and with concomitant hydrolysis of one of the nitrile groups.[25] Thermal cyclization of **3** (40−90% yields) and subsequent oxidation of the resulting 1,2-dihydropyrazine derivatives **4** (80−90% yields) gave access to compounds **5** containing distinct *para*-substituted phenyl groups at positions 5 and 6 in the pyrazine ring. No examples of *meta*- and *ortho*-substituted derivatives were reported.

Exploring the reactivity of the DAMN-based benzylidene imines **1** containing hydroxyl substituents in the phenyl ring with aromatic aldehydes, we found that while *meta* and *para*

Received: March 9, 2022
Accepted: June 13, 2022
Published: June 24, 2022

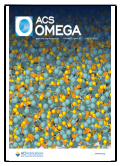

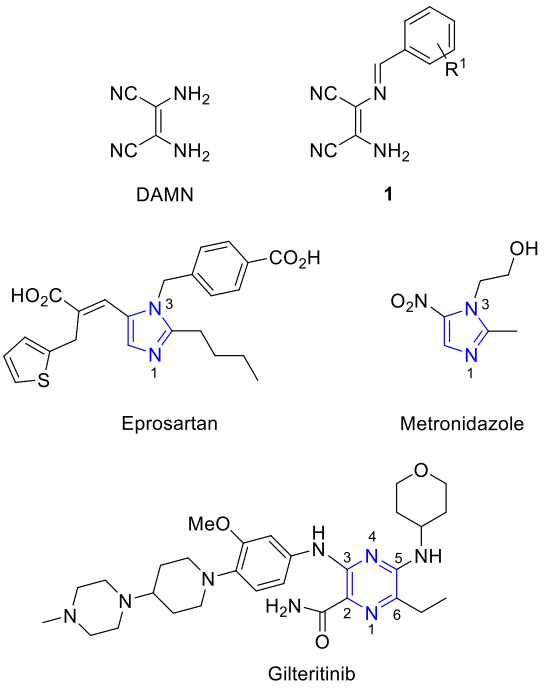

Figure 1. Examples of drugs in clinical use containing imidazole and pyrazine scaffolds and chemical structures of DAMN and DAMN-based benzylidene imines **1**.

Scheme 2. Synthetic Approach Explored in This Work

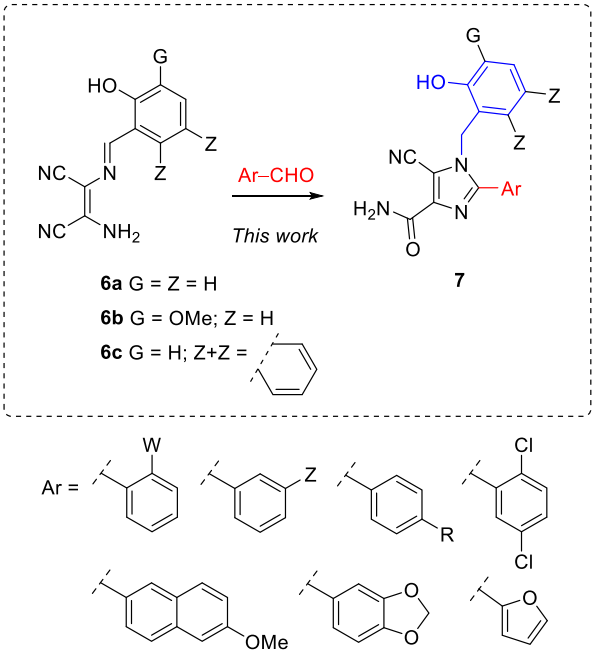

isomers give 1,2-dihydropyrazines **4**, the same does not happen with the corresponding ortho-substituted derivatives, compounds **6**, which afforded compounds **7** (Scheme 2). We report here a simple and efficient method for the regiocontrolled synthesis of a variety of 2-aryl-5-cyano-1-(2-hydroxyaryl)-1*H*-imidazole-4-carboxamides **7** from 2-hydroxybenzylidene imines **6**. The role of the 2-hydroxyaryl group in the regioselectivity of the reaction was also studied by computational studies on the reaction path.

RESULTS AND DISCUSSION

Synthesis of Compounds 7. First, the effect of the position of the hydroxyl substituent in the phenyl ring of the benzylidene imines was explored. To this end, the reactivity of the three possible isomers, compounds **6a**, **8**, and **9**, which

Scheme 1. Synthesis of Imidazoles 2 and Pyrazine Carboxamides 5 from DAMN-Based Benzylidene Imines 1[a]

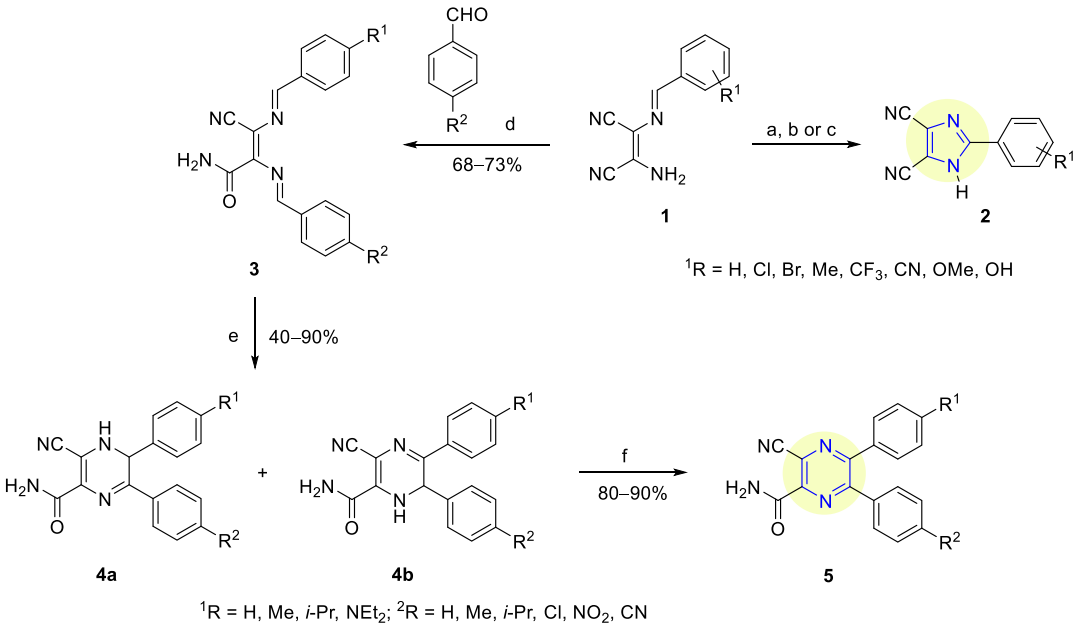

[a]Reagents, conditions, and yields: (a) MnO_2, EtOAc/MeCN, Δ, 50−70%; (b) nicotinamide, NCS, DMF, 50−60%; (c) CuO_x/OMS-2, DMA, 120 °C, 48−93%; (d) ArCHO, Et_3N, MeOH, EtOH, MeCN or PhH, −5 °C to RT; (e) DMSO, 80 °C; and (f) MnO_2, DMF, 60 °C or H_2O_2, MeOH, 50 °C.

https://doi.org/10.1021/acsomega.2c01399
ACS Omega 2022, 7, 23289−23301

were prepared as previously described,[9] with 2-chlorobenzaldehyde was studied (Figure 2). The reaction was performed

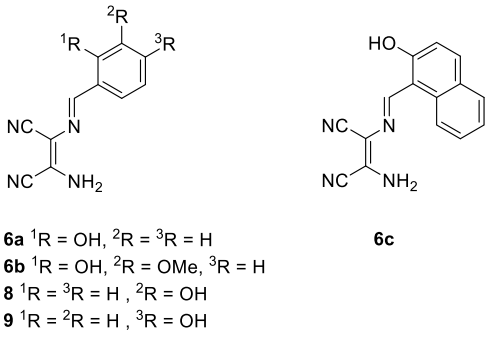

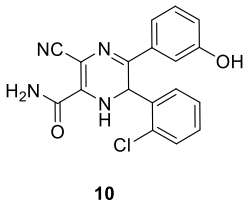

Figure 2. Hydroxybenzylidene imines explored in this work and the chemical structure of compound **10**, obtained using imine **8** and 2-chlorobenzaldehyde.

using 2 equiv of the aldehyde, in the presence of 2 equiv of triethylamine using ethanol as the solvent and at room temperature for 96 h. The results showed that the reaction performed with 2-hydroxybenzylidene imine **6a** gave mainly compound **7b**, while the formation of 1,2-dihydropyrazines was not experimentally observed. By contrast, for benzylidene imine **8**, a mixture of the corresponding diamine derivative **3** and 1,2-dihydropyrazines **4** was obtained, while the formation of the corresponding imidazole derivative was not detected. In addition, heating a deuterated dimethyl sulfoxide (DMSO-d_6) solution of the latter mixture at 80 °C for 30 min led to compound **10** as the only reaction product (Figure 2). Finally, the reaction carried out with imine **9** gave a complex mixture. The formation of compounds **7b** and **10** was corroborated by a combination of 1D (^{1}H, ^{13}C, and DEPT) and bidimensional (HMQC and HMBC) NMR experiments. For compound **7b**, the most remarkable NMR data are (i) the signals corresponding to the methylene group at 5.09 ppm (singlet, integration by two hydrogen atoms) and 46.2 ppm in the ^{1}H and ^{13}C NMR spectra, respectively, and (ii) the strong correlation signals of the methylene group with the CN group (110.7 ppm) and the quaternary carbon atom of the phenyl group (147.6 ppm) in the HMBC spectrum (see the Supporting Information for further details). The NMR spectra of compound **10** did not reveal the presence of a methylene group. Instead, a characteristic CH group is identified at 6.16 and 48.6 ppm in the ^{1}H and ^{13}C NMR spectra, respectively. Taken together, these outcomes revealed that the 2-phenol moiety in the DAMN-based imine **6a** seems to be essential for obtaining the imidazole carboxamides **7**.

The scope of the reaction was then explored using various aromatic aldehydes **11**, specifically benzaldehydes substituted with electron-withdrawing (Cl, Br, F, NO_2, and CN) and electron-donating (OMe and Me) groups, furan-2-carbaldehyde, 6-methoxy-2-naphthaldehyde, and piperonal (Scheme 3 and Table 1). The optimal experimental conditions were

Scheme 3. Synthesis of Imidazoles 7 from DAMN-Based Benzylidene Imines 6

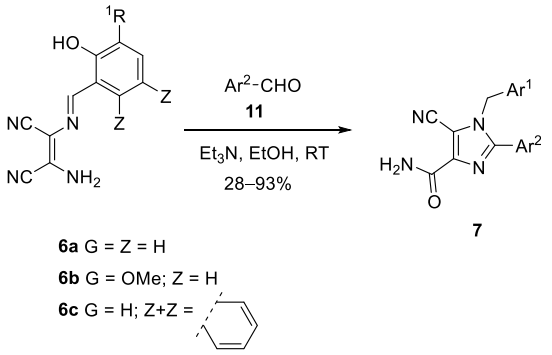

Table 1. Reaction Conditions and Yields for the Synthesis of 7[a]

comp.	Ar^1	Ar^2	time (h)	yield (%)
7a	2-OH-phenyl	phenyl	7	93
7b	2-OH-phenyl	2-Cl-phenyl	16	42
7c	2-OH-phenyl	3-Cl-phenyl	26	74
7d	2-OH-phenyl	4-Cl-phenyl	25	31
7e	2-OH-phenyl	2,5-(Cl)phenyl	17	37
7f	2-OH-phenyl	4-CN-phenyl	24	69
7g	2-OH-phenyl	3-Br-phenyl	19	73
7h	2-OH-phenyl	4-Br-phenyl	15	54
7i	2-OH-phenyl	3-F-phenyl	19	65
7j	2-OH-phenyl	4-tolyl	24	70
7k	2-OH-phenyl	2-OMe-phenyl	18	40
7l	2-OH-phenyl	3-NO_2-phenyl	15	89
7m	2-OH-phenyl	benzo[*d*](1,3]dioxol-5-yl	17	28
7n	2-OH-phenyl	6-OMe-naphthalen-2-yl	16	54
7o	2-OH-phenyl	furan-2-yl	24	53
7p	2-OH-3-OMe-phenyl	3-NO_2-phenyl	66	49
7q	2-OH-3-OMe-phenyl	2-Cl-phenyl	68	51
7r	2-OH-naphthalenyl	2-Br-phenyl	14	73

[a]1.2 equiv of **11** were used except for compounds **7a** (1.0 equiv), **7i** (1.5 equiv), and **7j** (1.5 equiv).

obtained using 1.0−1.5 equiv of aldehydes **11**, 2 equiv of triethylamine at room temperature, and ethanol as the solvent. Reaction times range from 7 to 68 h. In general, among the benzaldehydes employed, *meta*-substituted derivatives provided the best results with yields ranging from 73 to 89%. *Ortho*- and *para*-substituted benzaldehydes led to moderate yields (31−70%). The reaction was also shown to be useful for other aromatic aldehydes, and in this case, the yields varied according to the aldehyde that was used.

The reported method also proceeds satisfactorily using other substituted 2-hydroxybenzylidene imines such as **6b** or 2-hydroxyarylidene imines such as **6c** (Figure 2 and Table 1).

Altogether, the synthetic method reported here gives access, in a regiocontrolled manner, to a variety of highly substituted imidazole-4-carboxamides containing a 2-hydroxyarylidene group and an aryl group at positions 1 and 2, respectively.

Computational Studies. Having demonstrated that the presence of the 2-hydroxyphenyl moiety in the starting material is decisive in the regioselective synthesis of imidazoles **7**, the reaction mechanism was studied *in silico* to further explore its role in product formation. The calculations were performed assuming that the formation of the five-membered

https://doi.org/10.1021/acsomega.2c01399
ACS Omega 2022, 7, 23289−23301

Scheme 4. Schematic Representation of (A) the Intramolecular Cyclization Step for the Formation of Five- (Path a) and Six-Membered (Path a) Structures B and C, Respectively, and (B) the Aromatization Step Assisted by the 2-Phenol Group[a]

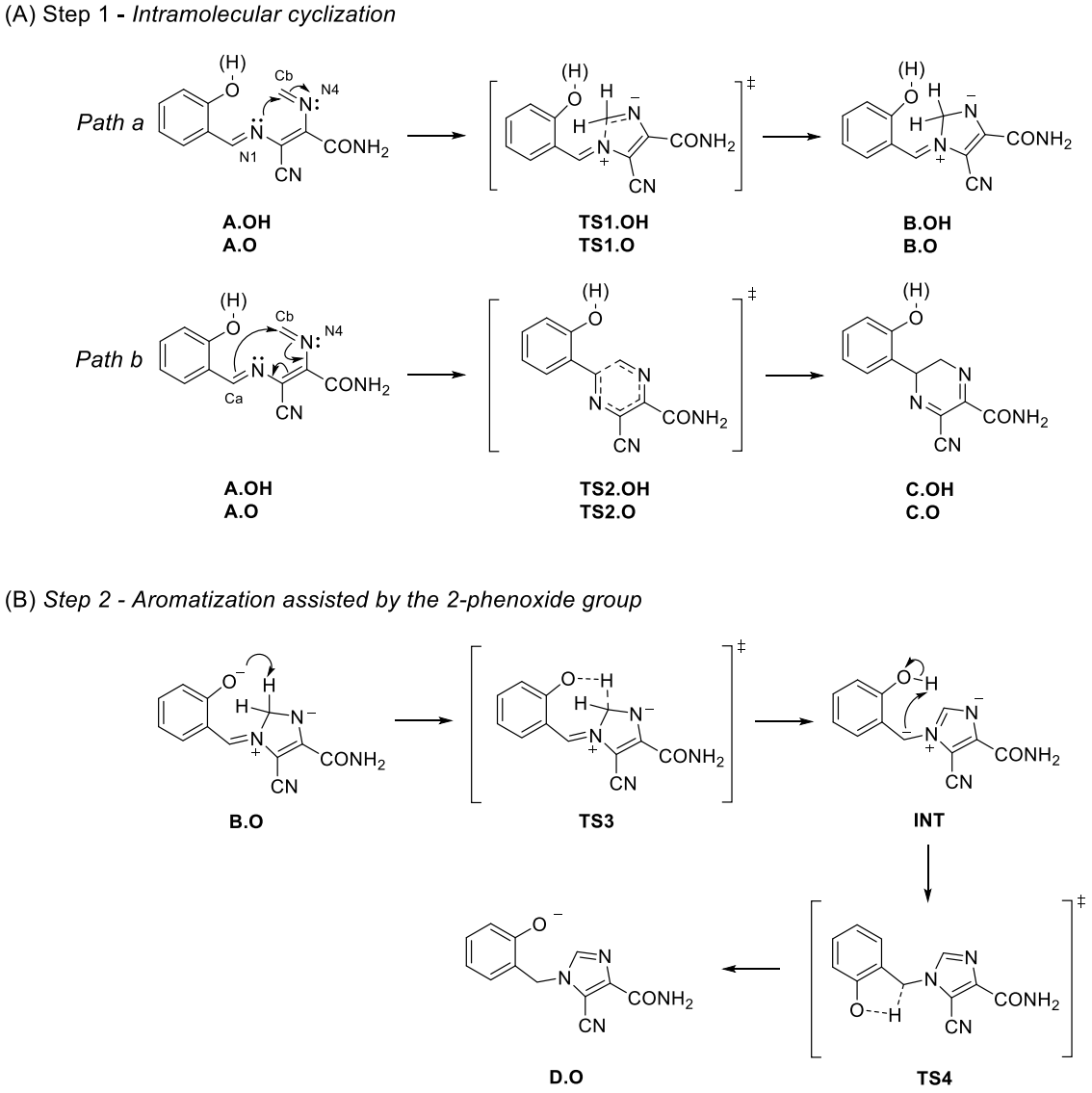

[a]The two plausible protonation states of the phenol group were considered for step 1 and are indicated with "**.OH**" (neutral form) and with "**.O**" (phenoxide form).

ring (that further leads to the final product **7**, path a) is started by the nucleophilic attack of the nitrogen atom (N1) of the 2-hydroxybenzylidene moiety to the carbon atom (Cb) of the *in situ* formed diimine, and the formation of the six-membered ring (that further leads to 1,2-dihydropyrazines, path b) occurs through an aza-Claisen-like rearrangement by the reaction between the two carbon atoms of the imine moieties (Ca and Cb) (Scheme 4). For our initial studies, the aryl group was not modulated and was substituted by a hydrogen atom. Once the reaction path was determined, the effect of the phenyl group was then explored, which will be discussed later.

Two main steps were considered: (1) intramolecular cyclization of the 2-hydroxybenzylidene structure **A** into the five-membered ring structure **B** (path a) and six-membered ring structure **C** (path b) (Scheme 4A) and (2) aromatization of structure **B** into the final imidazole form **D**, intramolecularly assisted by the 2-phenol moiety in the process (Scheme 4B).

Considering that the reaction conditions for the formation of either imidazoles or 1,2-dihydropyrazines involve the use of triethylamine, the two plausible protonation states of the phenol group were considered and are indicated with "**.OH**" (neutral form) and with "**.O**" (phenoxide form). Intrinsic reaction coordinate (IRC) calculations were performed to identify the transition states of each process.[25] All calculations were performed in the implicit solvent [CPMC (conductor-like polarizable continuum model,[26] ethanol] using program Gaussian 09[27] at the B3LYP level of theory with Grimme's correction[28] and the basis set TZVP.[29]

(1) Step 1—intramolecular cyclization: this was explored with the three possible isomers in the hydroxybenzylidene moiety (*ortho*, *meta*, and *para*) (see the Supporting Information). Both paths led to the respective transition states **TS1** and **TS2** in both protonation states studied (Figure 3A). When the neutral form was considered, an activation free energy barrier of 9.2 kcal mol^{-1} was obtained for the formation

https://doi.org/10.1021/acsomega.2c01399
ACS Omega 2022, 7, 23289−23301

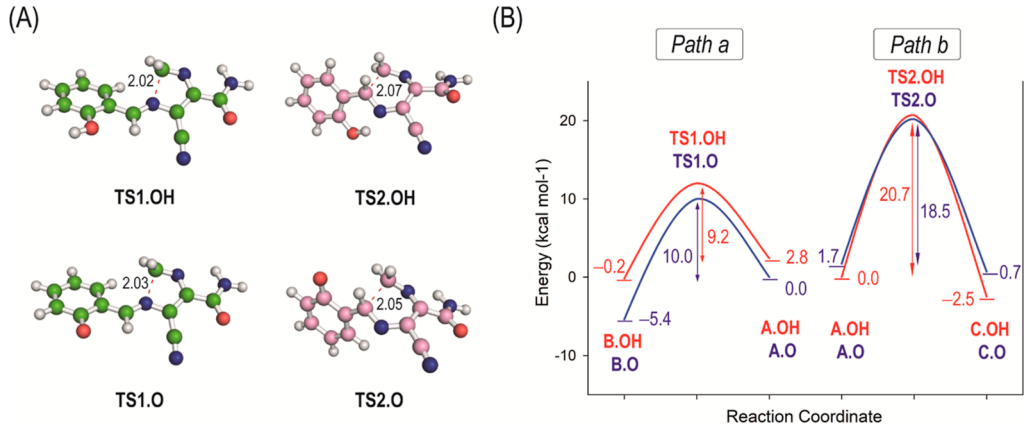

Figure 3. (A) Geometries of the transition states **TS1.OH**, **TS1.O**, **TS2.OH**, and **TS2.O** obtained by computational studies. (B) Free energy profiles for the cyclization steps (paths a and b) to afford five- and six-membered derivatives substituted with a 2-phenol group. The two plausible protonation states of the phenol group were considered and are indicated with "**.OH**" (neutral form) and with "**.O**" (phenoxide form). For better comparison of the energy barriers of the cyclization processes, the energy of the most suitable conformer of **A.OH** and **A.O** that leads to the corresponding transition state is given.

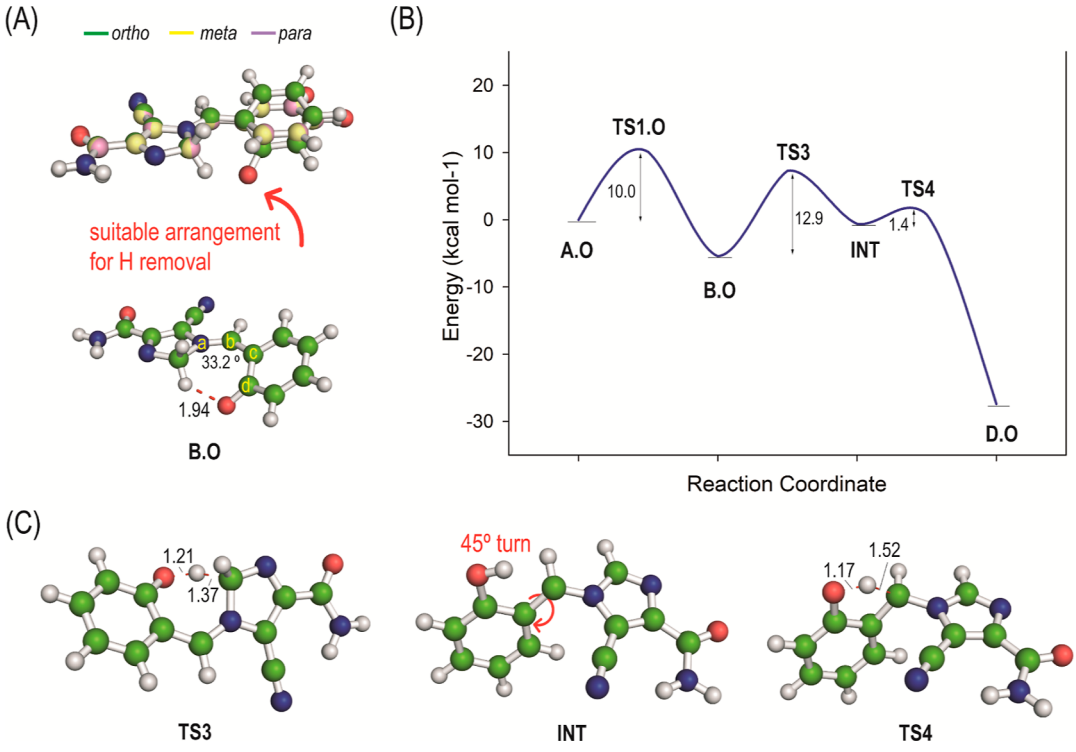

Figure 4. (A) Superposition of the geometries of the **B.O** intermediates in the three isomeric forms obtained by computational studies. Detailed view of the **B.O** intermediate of the ortho isomer highlighting the dihedral angle between the two rings. The atoms involved in the dihedral angle are highlighted. Note how for the meta and para isomers, both rings are coplanar. The non-coplanar arrangement of the ortho isomer as well as the proximity of the phenoxide group would facilitate the intramolecular removal of the hydrogen atom in the five-membered ring. (B) Free energy profiles for the formation of imidazole derivatives substituted with a 2-phenol group. Only the phenoxide forms of the starting material, intermediates, and transition states are considered. (C) Geometries of the transition states **TS3** and **TS4** and intermediate **INT** obtained by computational studies. Note how the intermediate **INT** undergoes a ∼45° turn to transfer the hydrogen atom.

of the five-membered compound **B**, while a value of 20.7 kcal mol^{-1} was obtained for the formation of the six-membered derivative **C** (Figure 3B). The energy differences between both paths were when the phenoxide form was employed (∼8 kcal mol^{-1}). For the three isomers, the formation of five-membered derivatives is predicted to be more favorable than the formation of six-membered ones (Figure S1). While no remarkable differences were obtained among the three isomers when the neutral form was used, a different scenario was obtained for the anionic form. Thus, while for the para isomer, the differences in activation energy values between both paths were similar to that of the ortho isomer (∼6−7 kcal mol^{-1}), for the *meta* isomer, the differences between the paths were higher (∼13 kcal mol^{-1}). These findings highlighted a strong contribution of the electronic effects on the intramolecular cyclization step, and based on the low energy barriers differences obtained, both paths would be possible and reversible. Therefore, the explanation for the different

https://doi.org/10.1021/acsomega.2c01399
ACS Omega 2022, 7, 23289−23301

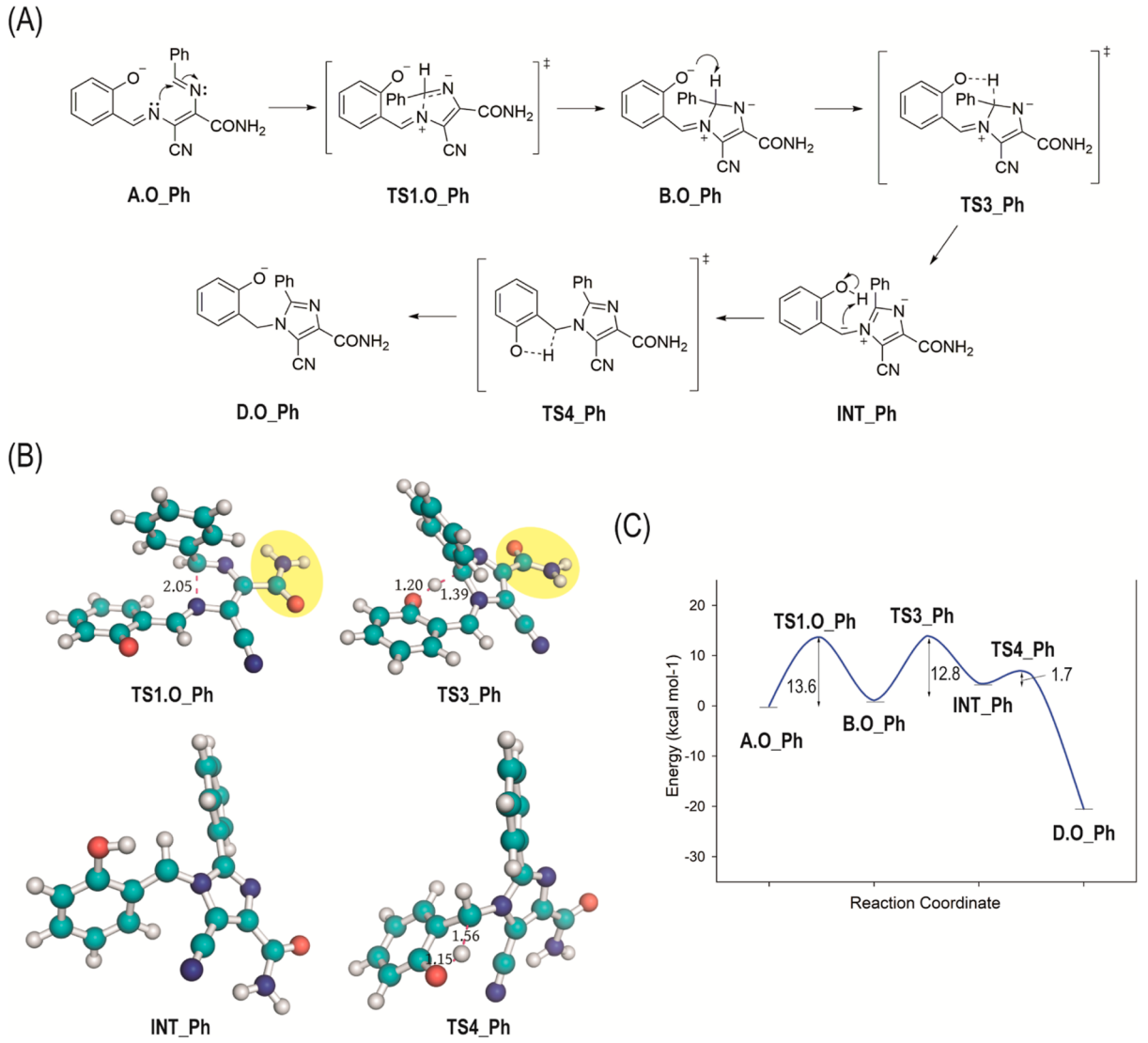

Figure 5. (A) Schematic representation of the intramolecular cyclization and aromatization steps assisted by the 2-phenol group to afford 1-(2-hydroxyphenyl)-2-phenyl imidazole derivatives; (B) geometries of the transition states **TS1.O_Ph**, **TS3_Ph**, and **TS4_Ph** and the intermediate **INT_Ph** obtained by computational studies; and (C) free energy profiles for the formation of 1-(2-hydroxyphenyl)-2-phenyl imidazole derivatives. Only the phenoxide forms of the starting material, intermediates, and transition states are considered. Note the different arrangement of the $CONH_2$ group in **TS1.O_Ph**, in which the NH_2 group is pointing toward the imine moiety (yellow shadow), from that in transition states **TS3_Ph** and **TS4_Ph** and intermediate **INT_Ph**.

regioselectivities obtained may lie in the subsequent evolution of the intermediates generated in this step.

On the other hand, the analysis of the transition states **TS1.OH**/**TS1.O** and **TS2.OH**/**TS2.O** revealed that for all the transition states, the NH_2 group of the amide moiety would be pointing toward the N4 nitrogen atom to establish an intramolecular hydrogen bonding interaction (Figures 3A and S2). This contact seems to help in achieving the best arrangement for cyclization. In addition, some differences among the TS1 structures, for the three isomers explored, were identified. Thus, the relative arrangement of the phenolic ring in relation to the five-membered structures, formed in the cyclization process, was shown to be distinct for the ortho isomer when compared with that for the meta and para isomers, which followed a similar architecture. For the *ortho* isomer, the phenolic ring showed to be almost coplanar to the new five-membered ring generated.

(2) Step 2—aromatization: an inspection of intermediates **B.OH** and **B.O**, which were obtained in step 1, showed remarkable differences in their spatial disposition depending on the position of the substituent in the aromatic ring (Figure 4A). Thus, for the *meta* and *para* isomers, an overall planar arrangement was mainly obtained with the newly formed five-membered ring and the phenol moiety in the same plane. However, for the *ortho* isomers, in which the substituent is located on the same site of the methylene group, the phenol/phenoxide ring is mainly arranged about 45 and 30°, respectively, from the coplanar disposition. The optimal conformation of **B.O** (*ortho*) to reach the transition state is shown. As a result, the oxygen atom in the phenol/phenoxide moiety would be close to one of the hydrogen atoms in the methylene group of the five-membered ring, with distances of 2.1 and 1.9 Å for the phenol and phenolate derivatives, respectively. Although there is free rotation around the C(sp2)−C(sp2, aryl) bond, this suitable arrangement for the

https://doi.org/10.1021/acsomega.2c01399
ACS Omega 2022, 7, 23289−23301

ortho intermediates **B.OH** and **B.O** suggests that the phenol/phenoxide moiety could be involved in the final aromatization of the five-membered ring generated to afford the experimentally observed imidazole derivatives. These findings led us to explore this intramolecular abstraction reaction, which would be geometrically difficult for the meta and para isomers (Figure S3). The fact that the velocity of the reaction was not increased with the concentration of the base also supported an intramolecular reaction mechanism.

As intermediate **B.OH** could also be converted into **B.O** by the reaction with the Et_3N employed in the reaction, our next calculations were focused on intermediate **B.O**. The full energy landscape is presented in Figure 4B. The calculated activation free energy barrier for the intramolecular hydrogen atom abstraction that led to transition state **TS3** and intermediate **INT** was 12.9 kcal mol^{-1} (Figure 4C). As a result of this reaction, the five-membered ring became flat, and a 45° turn in the resulting 2-phenol moiety was observed to locate the OH group close to the carbon atom that joins both rings, achieving a suitable arrangement for proton transfer. In the transition state of the latter process, **TS4**, the transferred proton was located at 1.52 Å to the benzylic carbon atom and at 1.17 Å to the phenolic oxygen atom. This step is expected to be very fast as the calculated activation free energy barrier was 1.4 kcal mol^{-1}. In addition, this step should be irreversible as the reverse process would have a high energy barrier of 26.8 kcal mol^{-1}. In contrast with that for **TS1.O** and **TS3**, for **TS4**, the carbonyl group of the amide group was pointing toward the heterocyclic nitrogen atom.

From the full energy landscape obtained for diimine **A.O**, we can conclude that the cyclization reactions for the formation of both the five- and six-membered ring derivatives show the following characteristics: (i) they are energetically favorable and (ii) as both reactions have relatively close energy barriers (of 10.0 and 18.5 kcal mol^{-1}, respectively), they are competitive processes and reversible. In addition, for the 3- and 4-hydroxybenzylidene derivatives **8** and **9**, since the generated five-membered intermediates **B.OH**/**B.O** cannot evolve, the process reverses, favoring the formation of the six-membered systems. However, for the ortho derivative **6**, as this type of substitution promotes the intramolecular abstraction of one of the methylene hydrogen atoms of the five-membered system **B.O**, the evolution of the reaction toward the formation of imidazole derivatives is triggered. The low energy barriers of the abstraction and protonation steps, and an $\Delta G^{\ddagger}$ calculated for the global process leading to the imidazole derivative **D.O** to be −27.4 kcal mol^{-1}, would make this reaction highly favorable in comparison to the formation of the six-membered derivative.

Finally, following a similar approach, the effect of the presence of a phenyl group in the *in situ* generated diamine derivative (such as **3**) was evaluated by studying the conversion of diimine **A.O_Ph** into imidazole **D.O_Ph** (Figure 5). The results showed that the overall process would also be energetically favorable with an $\Delta G^{\ddagger}$ calculated to be −20.5 kcal mol^{-1} and energy barriers of 13.6 and 12.8 kcal mol^{-1} for the first and second steps, respectively. According to the calculations performed here, while no significant differences were identified for the second step (intramolecular H abstraction), the energy barrier involving the intramolecular cyclization leading to the formation of the five-membered ring would be 3.6 kcal mol^{-1} higher, probably because of the stereo hindrance introduced by the substitution of a hydrogen atom by a phenyl group. No relevant differences were identified in the geometries and arrangements of the transition states and intermediates. In addition, the energy activation barriers differences for the formation of five- and six-membered rings were revealed to be smaller, which reinforces the idea of competitive processes (Figure S4).

CONCLUSIONS

A series of 2-aryl-5-cyano-1-(2-hydroxybenzyl)-1*H*-imidazole-4-carboxamides **7** were regioselectively prepared from DAMN-based benzylidene imines **6** and diverse aromatic aldehydes **11**. Exploring the reaction mechanism that led to their formation showed that the presence of the 2-hydroxyaryl moiety controls the mechanism of the reaction, guiding it mainly through a self-catalyzed hydrogen atom shift. These conclusions were based on the reactions performed with hydroxybenzylidene imines **6**, **8**, and **9**, where it was observed that (i) only the imines possessing a 2-hydroxyl moiety in the aromatic ring, compounds **6**, evolved to imidazoles **7**, while imines **8** (3-OH) and **9** (4-OH) led to the formation of pyrazines **4**, much likely *via* a diaza-Cope rearrangement. The mechanism of the regioselective formation of imidazoles **7** was supported by computational studies, where the most energetically favorable process involved a phenol-assisted hydrogen atom shift, which is not geometrically suitable for the corresponding *meta* and *para* derivatives.

EXPERIMENTAL SECTION

General. All chemicals and solvents for synthesis were of the analytical grade, purchased from commercial sources and used without further purification, unless otherwise specified. The reactions were monitored by thin layer chromatography, using glass plates precoated with silica gel 60 and a fluorescent indicator (Macherey Nagel, DC-Fertigplatten Duresil 25 UV254) or aluminum plates precoated with silica gel 60 and a fluorescent indicator (Macherey Nagel, DC-Fertigfolien ALUGRAM Xtra SIL G/UV254). The spots were observed under ultraviolet (UV) light irradiation in a UV chamber (CN-6 Vilber Lourmat) with a 254 nm lamp and in an iodine chamber. For flash chromatography, silica gel MN Kieselgel 60 (230 ASTM, particle size <0.063 mm) was used. Distilled water was used in the reactions performed in aqueous solution. The NMR spectra were recorded at room temperature on a Varian Unity Plus spectrometer (^{1}H: 300 MHz and ^{13}C: 75 MHz) or a Brucker AVANCE III spectrometer (^{1}H: 400 MHz, 500 MHz and ^{13}C: 100 MHz, 125 MHz), using DMSO-d_6 as the solvent. The chemical shifts (δ) are expressed in parts per million (ppm), and the coupling constants (J) are given in hertz (Hz). NMR assignments were obtained by a combination of 1D and bidimensional (HMQC and HMBC) experiments. IR spectra were recorded on a Fourier transform infrared (FTIR) Bomem MB apparatus with Nujol mulls or NaCl plates or on a PerkinElmer Two FTIR spectrometer with attenuated total reference (ATR). Melting points were determined using a Stuart SMP3 melting point apparatus or a Büchi M-560 apparatus. Electrospray ionization (ESI) mass spectra were recorded on a Bruker BIOTOF II mass spectrometer. Elemental analysis was determined on a Thermo Flash EA 1112 (NC Soil Analyzer) apparatus [carrier gas flux (He): 130 mL/min; reference gas flux (He): 100 mL/min; oxygen flux: 250 mL/min; oven temperature: 950 °C; column: multiple analysis 6 × 5 mm, 2.0 m de Cromlab; column

https://doi.org/10.1021/acsomega.2c01399
ACS Omega 2022, 7, 23289−23301

temperature: 75 °C.; and standard: sulfanilamide (Thermo Scientific)]. Hydroxybenzylidene imines **6a**, **8**, and **9** were prepared as previously described.[9]

*2-Amino-3-(((E)-2-hydroxy-3-methoxybenzylidene)-amino)malenonitrile (**6b**).* DAMN (0.54 g, 5.0 mmol) and 3-methoxy salicylaldehyde (0.76 g, 5.0 mmol) were combined in the minimum amount of DMSO and treated with a catalytic amount of H_2SO_4 (c), and the resulting mixture was vigorously stirred for 3 min. A solid precipitate was generated almost instantaneously. The reaction mixture was diluted with water (15 mL), and the dense suspension was cooled in an ice bath for 2 h. The solid was filtered, and the filtrate was successively washed with water, ethanol, and diethyl ether and dried. Dark-yellow solid (1.19 g, 98%). mp 221 °C (dec). ^{1}H NMR (400 MHz, DMSO-d_6): δ/ppm 9.86 (s, 1H, OH), 8.59 (s, 1H, NCHAr), 7.84 (s, 2H, NH_2), 7.61 (dd, J_1 = 7.6, J_2 = 1.2 Hz, 1H, H6′), 7.06 (dd, J_1 = 7.6, J_2 = 1.2 Hz, 1H, H4′), 6.83 (t, J = 8.0 Hz, 1H, H5′), and 3.83 (s, 3H, OMe). IR (nujol) $\overline{\nu}$/cm^{-1}: 3408 (s), 3324 (s), 3208 (w), 2245 (m), 2205 (m), 1645 (s), 1602 (s), 1589 (m), and 1526 (w). MS (ESI) m/z: 243 (MH^+). HRMS calcd for $C_{12}H_{10}N_4O_2$ (MH^+), 243.0877; found, 243.0872.

*2-Amino-3-(((E)-2-hydroxynaphthalen-1-yl)methylene)-amino)malenonitrile (**6c**).* This compound was prepared following a similar procedure to that used for **6b**. Yellow solid (92%). mp 223−225 °C. ^{1}H NMR (500 MHz, DMSO-d_6): δ/ppm 11.96 (s, 1H, OH), 9.24 (s, 1H, NCHAr), 8.60 (d, J = 8.6 Hz, 1H, H8′), 7.98 (d, J = 8.9 Hz, 1H, H4′), 7.87 (d, J = 8.5 Hz, 1H, H5′), 7.86 (s, 2H, NH_2), 7.61 (t, J = 8.5 Hz, 1H, H7′), 7.41 (t, J = 8.5 Hz, 1H, H6′), and 7.22 (d, J = 9.0 Hz, 1H, H3′). ^{13}C NMR (125 MHz, DMSO-d_6): δ/ppm 159.8 (C2′), 154.9 (NCHAr), 135.2 (C4′), 131.7 (C8a′), 128.9 (C5′), 128.5 (C7′), 127.8 (C4a′), 125.1 (C1), 123.9 (C6′), 121.9 (C8′), 118.5 (C3′), 114.6 (CN), 114.1 (CN), 110.2 (C1′), and 103.9 (C2). IR (ATR) $\overline{\nu}$/cm^{-1}: 3466 (m), 3340 (m), 3194 (m), 2242 (m), 2197 (m), 1618 (s), 1603 (m), 1557 (m), and 1356 (m). MS (ESI) m/z: 263 (MH^+). HRMS calcd for $C_{15}H_{11}N_4O$ (MH^+), 263.0927; found, 263.0925.

General Procedure for the Synthesis of Imidazoles 7. A suspension of the 2-hydroxybenzylidene imine **6a**[9] in ethanol (2 mL, 0.45 M) was treated with aromatic aldehydes 11 (1.0−1.5 equiv) and Et_3N (2 equiv), and the reaction mixture was stirred at room temperature for 7−24 h. The resulting suspension was then cooled in an ice bath for 2 h, and the obtained precipitate was filtered, successively washed with cold methanol or ethanol and diethyl ether, and dried.

*5-Cyano-1-(2-hydroxybenzyl)-2-phenyl-1H-imidazole-4-carboxamide (**7a**).* Light-brown solid (93%). mp 227−229 °C. ^{1}H NMR (400 MHz, DMSO-d_6): δ/ppm 9.91 (s, 1H, OH), 7.65 (s, 1H, CONHH), 7.80 (s, 1H, CONHH), 7.60 (dd, J_1 = 7.6 Hz, J_2 = 1.6 Hz, 2H, H2″ + H6″), 7.50 (t, J = 8.0 Hz, 1H, H4″), 7.48 (dt, J_1 = 7.6 Hz, J_2 = 1.2 Hz, 2H, H3″ + H5″), 7.11 (dt, J_1 = 8.0 Hz, J_2 = 1.6 Hz, 1H, H4′), 6.80 (dd, J_1 = 8.0 Hz, J_2 = 0.8 Hz, 1H, H3′), 6.70 (dt, J_1 = 7.6 Hz, J_2 = 1.2 Hz, 1H, H5′), 6.56 (dd, J_1 = 7.6 Hz, J_2 = 1.6 Hz, 1H, H6′), and 5.28 (s, 2H, CH_2). ^{13}C NMR (100 MHz, DMSO-d_6): δ/ppm 161.5 (CO), 154.5 (C2′), 150.5 (C2), 144.0 (C4), 130.3 (C4″), 129.2 (C4′), 128.9 (C2″ + C6″), 128.7 (C3″ + C5″), 128.4 (C1″), 127.0 (C6′), 121.3 (C1′), 119.1 (C5′), 115.1 (C3′), 110.9 (CN), 107.7 (C5), and 46.2 (CH_2). IR (nujol) $\overline{\nu}$/cm^{-1}: 3473 (m), 3365 (m), 3328 (m), 2231 (m, CN), 1686 (s, CO), 1669 (m), and 1591 (m). Elemental analysis calcd for $C_{18}H_{14}N_4O_2$: C, 67.91; H, 4.43; N, 17.60. Found: C, 67.77; H, 4.36; N, 17.59.

*2-(2-Chlorophenyl)-5-cyano-1-(2-hydroxybenzyl)-1H-imidazole-4-carboxamide (**7b**).* Light-pink solid (42%). mp 230−232 °C. ^{1}H NMR (400 MHz, DMSO-d_6): δ/ppm 9.81 (s, 1H, OH), 7.61 (s, 1H, CONHH), 7.80 (s, 1H, CONHH), 7.57 (t, J = 7.6 Hz, 1H, H4″), 7.55 (dd, J_1 = 7.6 Hz, J_2 = 2.0 Hz, 1H, H3″), 7.45 (dt, J_1 = 8.0 Hz, J_2 = 1.6 Hz, 1H, H5″), 7.43 (dd, J_1 = 8.0 Hz, J_2 = 2.0 Hz, 1H, H6″), 7.06 (dt, J_1 = 8.0 Hz, J_2 = 0.8 Hz, 1H, H4′), 6.71 (dd, J_1 = 8.0 Hz, J_2 = 0.8 Hz, 1H, H3′), 6.58 (dt, J_1 = 7.6 Hz, J_2 = 0.8 Hz, 1H, H5′), 6.49 (dd, J_1 = 7.6 Hz, J_2 = 1.2 Hz, 1H, H6′), and 5.09 (s, 2H, CH_2). ^{13}C NMR (100 MHz, DMSO-d_6): δ/ppm 161.4 (CO), 155.1 (C2′), 147.6 (C2), 143.6 (C4), 133.4 (C1″), 132.3 (C4″, C5″), 129.6 (C3″), 129.5 (C4′), 128.6 (C6′), 127.8 (C2″), 127.3 (C6″), 120.4 (C1′), 118.6 (C5′), 115.0 (C3′), 110.7 (CN), 107.5 (C5), and 46.2 (CH_2). IR (nujol) $\overline{\nu}$/cm^{-1}: 3477 (m), 3348 (m), 2238 (m, CN), 1668 (s, CO), and 1599 (m). Elemental analysis calcd for $C_{18}H_{13}ClN_4O_2$: C, 61.28; H, 3.71; N, 15.88. Found: C, 61.57; H, 3.62; N, 16.07.

*2-(3-Chlorophenyl)-5-cyano-1-(2-hydroxybenzyl)-1H-imidazole-4-carboxamide (**7c**).* Light-pink solid (74%). mp 230 °C (dec). ^{1}H NMR (400 MHz, DMSO-d_6): δ/ppm 9.98 (s, 1H, OH), 7.65 (s, 1H, CONHH), 7.83 (s, 1H, CONHH), 7.68 (t, J = 7.6 Hz, 1H, H2″), 7.57 (dt, J_1 = 8.4 Hz, J_2 = 1.2 Hz, 1H, H5″), 7.53 (d, J = 8.4 Hz, 1H, H6″), 7.51 (d, J = 8.0 Hz, 1H, H4″), 7.11 (dt, J_1 = 8.8, J_2 = 1.6 Hz, 1H, H4′), 6.78 (dd, J_1 = 8.0, J_2 = 0.4 Hz, 1H, H3′), 6.70 (dt, J_1 = 8.0, J_2 = 0.4 Hz, 1H, H5′), 6.65 (dd, J_1 = 7.6, J_2 = 1.2 Hz, 1H, H6′), and 5.31 (s, 2H, CH_2). ^{13}C NMR (100 MHz, DMSO-d_6): δ/ppm 161.5 (CO), 154.8 (C2′), 149.0 (C2), 144.0 (C4), 133.5 (C3″), 130.7 (C4″), 130.5 (C1″), 130.3 (C5″), 129.5 (C4′), 128.9 (C2″), 127.8 (C6′), 127.5 (C6″), 121.0 (C1′), 119.1 (C5′), 115.0 (C3′), 110.8 (CN), 108.2 (C5), and 46.5 (CH_2). IR (nujol) $\overline{\nu}$/cm^{-1}: 3479 (m), 3369 (m), 3331 (m), 2233 (m, CN), 1685 (s, CO), 1670 (m), and 1590 (m). Elemental analysis calcd for $C_{18}H_{13}ClN_4O_2$: C, 61.28; H, 3.71; N, 15.88. Found: C, 61.26; H, 3.62; N, 16.07.

*2-(4-Chlorophenyl)-5-cyano-1-(2-hydroxybenzyl)-1H-imidazole-4-carboxamide (**7d**).* Light-pink solid (31%). mp 208−210 °C. ^{1}H NMR (400 MHz, DMSO-d_6): δ/ppm 9.90 (s, 1H, OH), 7.65 (s, 1H, CONHH), 7.81 (s, 1H, CONHH), 7.63 (dd, J_1 = 8.8, J_2 = 2.0 Hz, 2H, H2″ + H6″), 7.57 (dd, J_1 = 8.8, J_2 = 2.0 Hz, 2H, H3″ + H5″), 7.10 (dt, J_1 = 8.0, J_2 = 0.8 Hz, 1H, H4′), 6.78 (dd, J = 8.0, J_2 = 0.4 Hz, 1H, H3′), 6.69 (dt, J_1 = 7.2, J_2 = 0.8 Hz, 1H, H5′), 6.52 (dd, J_1 = 7.6, J_2 = 1.2 Hz, 1H, H6′), and 5.29 (s, 2H, CH_2). ^{13}C NMR (100 MHz, DMSO-d_6): δ/ppm 161.5 (CO), 154.7 (C2′), 149.4 (C2), 144.0 (C4), 135.2 (C4″), 130.8 (C3″+ C5″), 129.4 (C4′), 128.9 (C2″+ C6″), 127.5 (C6′), 127.4 (C1″), 121.0 (C1′), 119.0 (C5′), 115.1 (C3′), 110.8 (CN), 108.0 (C5), and 46.3 (CH_2). IR (nujol) $\overline{\nu}$/cm^{-1}: 3605 (m), 3513 (m), 3369 (m), 3439 (m), 2230 (m, CN), 1688 (s, CO), and 1604 (s). Elemental analysis calcd for $C_{18}H_{13}ClN_4O_2{\cdot}H_2O$: C, 58.31; H, 4.08; N, 15.11. Found: C, 58.44; H, 4.06; N, 15.09.

*2-(2,5-Dichlorophenyl)-5-cyano-1-(2-hydroxybenzyl)-1H-imidazo-le-4-carboxamide (**7e**).* Light-brown solid (37%). mp 225−227 °C. ^{1}H NMR (400 MHz, DMSO-d_6): δ/ppm 9.47 (s, 1H, OH), 7.57 (s, 1H, CONHH), 7.76 (s, 1H, CONHH), 7.60 (dd, J_1 = 8.8, J_2 = 2.4 Hz, 1H, H3″), 7.57 (d, J = 8.4 Hz, 1H, H4″), 7.50 (d, J = 2.4 Hz, 1H, H6″), 6.58 (d, J = 8.0 Hz, 1H, H6′), 6.70 (d, J = 7.6 Hz, 1H, H3′), 7.07 (m, 1H, H4′), 6.57 (d, J = 8.0 Hz, 1H, H5′), and 5.09 (s, 2H, CH_2).

https://doi.org/10.1021/acsomega.2c01399
ACS Omega 2022, 7, 23289−23301

^{13}C NMR (100 MHz, DMSO-d_6): δ/ppm 161.8 (CO), 155.6 (C2′), 146.6 (C2), 143.7 (C4), 132.7 (C3″), 132.5 (C4″), 132.2 (C6″), 132.1 (C2″), 131.6 (C5″), 130.2 (C4′), 129.8 (C1″), 129.7 (C6′), 120.4 (C1′), 119.0 (C5′), 115.4 (C3′), 110.8 (CN), 108.2 (C5), and 46.5 (CH_2). IR (nujol) $\overline{\nu}$/cm^{-1}: 3477 (m), 3370 (m), 3284 (m), 2233 (m, CN), 1666 (s, CO), and 1585 (m). Elemental analysis calcd for $C_{18}H_{12}Cl_2N_4O_2$: C, 55.83; H, 3.12; N, 14.47. Found: C, 55.74; H, 3.19; N, 14.41.

*5-Cyano-2-(4-cyanophenyl)-1-(2-hydroxybenzyl)-1H-imidazole-4-carboxamide (**7f**).* Gray solid (69%). mp 199−201 °C. ^{1}H NMR (400 MHz, DMSO-d_6): δ/ppm 9.91 (s, 1H, OH), 7.97 (d, J = 8.0 Hz, 2H, H3″ + H5″), 7.67 (s, 1H, CONHH), 7.84 (s, 2H, CONHH), 7.81 (d, J = 8.0 Hz, 2H, H2″ + H6″), 7.10 (m, 1H, H4′), 6.76 (d, J = 8.0 Hz, 1H, H3′), 6.68 (d, J = 4.4, 2H, H5′, H6′), and 5.09 (s, 2H, CH_2). ^{13}C NMR (100 MHz, DMSO-d_6): δ/ppm 161.4 (CO), 154.9 (C2′), 148.7 (C2), 144.2 (C4), 133.0 (C1″), 132.7 (C3″+ C5″), 129.8 (C2″ + C6″), 129.6 (C4′), 128.1 (C6′), 120.8 (C1′), 119.0 (C5′), 118.3 (CN), 112.7 (C4″), 115.2 (C3′), 110.7 (CN), 108.6 (C5), and 46.7 (CH_2). IR (nujol) $\overline{\nu}$/cm^{-1}: 3394 (m), 3344 (m), 2230 (m, CN), 2224 (m, CN), 1679 (s, CO), and 1597 (m). Elemental analysis calcd for $C_{19}H_{13}N_5O_2$: C, 66.47; H, 3.82. N, 20.40. Found: C, 66.50; H, 3.79; N, 20.56.

*2-(3-Bromophenyl)-5-cyano-1-(2-hydroxybenzyl)-1H-imidazole-4-carboxamide (**7g**).* Light-pink solid (73%). mp 220−222 °C. ^{1}H NMR (400 MHz, DMSO-d_6): δ/ppm 9.92 (s, 1H, OH), 7.65 (s, 1H, CONHH), 7.84 (s, 1H, CONHH), 7.83 (d, J = 1.6 Hz, 1H, H2″), 7.71 (dd, J_1 = 8.0, J_2 = 0.8 Hz, 1H, H6″), 7.60 (dd, J_1 = 8.0, J_2 = 1.2 Hz, 1H, H4″), 7.44 (t, J = 8.0 Hz, 1H, H5″), 7.11 (dt, J_1 = 8.0, J_2 = 2.0 Hz, 1H, H4′), 6.79 (d, J = 8.0 Hz, 1H, H3′), 6.71 (dt, J_1 = 7.6, J_2 = 1.2 Hz, 1H, H5′), 6.67 (dd, J_1 = 7.6, J_2 = 1.2 Hz, 1H, H6′), and 5.31 (s, 2H, CH_2). ^{13}C NMR (100 MHz, DMSO-d_6): δ/ppm 161.4 (CO), 154.8 (C2′), 148.8 (C2), 144.0 (C4), 133.1 (C6″), 131.7 (C2″), 130.8 (C5″), 130.7 (C1″), 129.4 (C4′), 127.8 (C4″), 127.7 (C6′), 121.8 (C3″), 121.0 (C1′), 119.0 (C5′), 115.1 (C3′), 110.8 (CN), 108.2 (C5), and 46.5 (CH_2). IR (nujol) $\overline{\nu}$/cm^{-1}: 3477 (m), 3367 (s), 2233 (m, CN), 1683 (m), 1668 (s, CO), and 1591 (s). Elemental analysis calcd for $C_{18}H_{13}BrN_4O_2$: C, 54.43; H, 3.30; N, 14.10. Found: C, 54.73; H, 3.27; N, 13.98.

*2-(4-Bromophenyl)-5-cyano-1-(2-hydroxybenzyl)-1H-imidazole-4-carboxamide (**7h**).* Light-pink solid (54%). mp 174−175 °C. ^{1}H NMR (400 MHz, DMSO-d_6): δ/ppm 9.89 (s, 1H, OH), 7.66 (s, 1H, CONHH), 7.81 (s, 1H, CONHH), 7.71 (dd, J_1 = 7.6, J_2 = 2.0 Hz, 2H, H2″ + H6″), 7.56 (dd, J_1 = 8.8, J_2 = 2.0 Hz, 2H, H3″ + H5″), 7.11 (dt, J_1 = 8.0, J_2 = 1.6 Hz, 1H, H4′), 6.78 (dd, J = 8.0, J_2 = 0.4 Hz, 1H, H3′), 6.69 (dt, J_1 = 7.6, J_2 = 0.8 Hz, 1H, H5′), 6.62 (dd, J_1 = 7.6, J_2 = 1.6 Hz, 1H, H6′), and 5.27 (s, 2H, CH_2). ^{13}C NMR (100 MHz, DMSO-d_6): δ/ppm 161.4 (CO), 154.7 (C2′), 149.4 (C2), 144.1 (C4), 139.9 (C2″+ C6″), 131.8 (C3″+ C5″), 129.3 (C4′), 127.7 (C1″), 127.5 (C6′), 123.9 (C4″), 121.0 (C1′), 119.0 (C5′), 115.1 (C3′), 110.8 (CN), 108.0 (C5), and 46.3 (CH_2). IR (nujol) $\overline{\nu}$/cm^{-1}: 3429 (m), 3352 (w), 3183 (m), 2224 (m, CN), 1687 (s, CO), and 1601 (s). Elemental analysis calcd for $C_{18}H_{13}BrN_4O_2{\cdot}0.7H_2O$: C, 52.75; H, 3.54; N, 13.67. Found: C, 52.57; H, 3.88; N, 13.39.

*2-(3-Fluorphenyl)-5-cyano-1-(2-hydroxybenzyl)-1H-imidazole-4-carboxamide (**7i**).* Light-brown solid (65%). mp >300 °C. ^{1}H NMR (400 MHz, DMSO-d_6): δ/ppm 9.90 (s, 1H, OH), 7.67 (s, 1H, CONHH), 7.82 (s, 1H, CONHH), 7.53 (dt, J_1 = 6.4 Hz, J_2 = 2.0 Hz, 1H, H5″), 7.45 (ddd, J_1 = 6.8, J_2 = 2.4 Hz, J_3 = 1.2 Hz, 2H, H2″, H6″), 7.37 (ddt, J_1 = 8.0, J_2 = 2.4 Hz, J_3 = 1.2 Hz, 1H, H4″), 7.11 (dt, J_1 = 8.0, J_2 = 1.6 Hz, 1H, H4′), 6.79 (dd, J_1 = 8.0, J_2 = 0.8 Hz, 1H, H3′), 6.69 (dt, J_1 = 7.6, J_2 = 1.2 Hz, 1H, H5′), 6.64 (dd, J_1 = 7.6, J_2 = 1.6 Hz, 1H, H6′), and 5.33 (s, 2H, CH_2). ^{13}C NMR (100 MHz, DMSO-d_6): δ/ppm 161.8 (d, J = 244.0 Hz, C3″), 161.4 (CO), 154.7 (C2, C2′), 145.0 (d, J = 3.0 Hz, C1″), 144.0 (C4), 130.9 (d, J = 8.0 Hz, C5″), 129.3 (C4′), 127.6 (C6′), 125.0 (d, J = 3.0 Hz, C6″), 121.0 (C1′), 119.0 (C5′), 117.2 (d, J = 21.0 Hz, C4″), 115.9 (d, J = 23.0 Hz, C2″), 115.1 (C3′), 110.8 (CN), 108.1 (C5), and 46.4 (CH_2). IR (nujol) $\overline{\nu}$/cm^{-1}: 3489 (m), 3379 (m), 3332 (m), 2233 (m, CN), 1682 (m), 1672 (s, CO), and 1591 (s). Elemental analysis calcd for $C_{18}H_{13}FN_4O_2$/336.32: C, 64.28; H, 3.90; N, 16.66. Found: C, 64.34; H, 3.79; N, 16.71.

*5-Cyano-1-(2-hydroxybenzyl)-2-(4-tolyl)-1H-imidazole-4-carboxamide (**7j**).* Brown solid (70%). mp 256−258 °C. ^{1}H NMR (400 MHz, DMSO-d_6): δ/ppm 9.82 (s, 1H, OH), 7.76 (s, 1H, CONHH), 7.59 (s, 1H, CONHH), 7.40 (dt, J_1 = 7.6, J_2 = 1.2 Hz, 1H, H3″ or H5″), 7.35 (dd, J_1 = 8.0, J_2 = 1.6 Hz, 1H, H2″ or H6″), 7.27 (t, J = 7.2 Hz, 2H, H3″ or H5″, H2″ or H6″), 7.07 (dt, J_1 = 7.6, J_2 = 0.8 Hz, 1H, H4′), 6.72 (dd, J_1 = 8.0, J_2 = 0.8 Hz, 1H, H3′), 6.59 (dt, J_1 = 7.6, J_2 = 0.8 Hz, 1H, H5′), 6.39 (dd, J_1 = 7.6, J_2 = 1.2 Hz, 1H, H6′), 5.07 (s, 2H, CH_2), and 1.95 (s, 3H, CH_3). ^{13}C NMR (100 MHz, DMSO-d_6): δ/ppm 161.6 (CO), 155.0 (C2′), 149.9 (C2), 143.3 (C4), 138.1 (C4″), 130.3 (C3″ or C5″), 130.2 (C3″ or C5″), 129.7 (C2″ or C6″), 129.6 (C2″ or C6″), 129.3 (C4′), 128.2 (C6′), 120.7 (C1′), 118.6 (C5′), 114.8 (C3′), 111.0 (CN), 107.2 (C5), 45.9 (CH_2), and 18.93 (CH_3). IR (nujol) $\overline{\nu}$/cm^{-1}: 3458 (m), 3295 (m), 3239 (m), 2233 (m, CN), 1658 (s, CO), and 1597 (m). Elemental analysis calcd for $C_{19}H_{16}N_4O_2$: C, 68.66; H, 4.85; N, 16.86. Found: C, 68.99; H, 4.85; N, 16.99.

*5-Cyano-1-(2-hydroxybenzyl)-2-(2-methoxyphenyl)-1H-imidazole-4-carboxamide (**7k**).* Light-orange solid (40%). mp 212−214 °C. ^{1}H NMR (400 MHz, DMSO-d_6): δ/ppm 9.81 (s, 1H, OH), 7.57 (s, 1H, CONHH), 7.74 (s, 1H, CONHH), 7.50 (dt, J_1 = 7.6 Hz, J_2 = 1.6 Hz, 1H, H4″), 7.28 (dd, J_1 = 7.6 Hz, J_2 = 1.6 Hz, 1H, H6″), 7.11 (d, J = 8.0 Hz, 1H, H3″), 7.00 (dt, J_1 = 7.2 Hz, J_2 = 0.8 Hz, 1H, H5″), 7.05 (dt, J_1 = 8.0, J_2 = 1.6 Hz, 1H, H4′), 6.71 (dd, J = 8.0, J_2 = 0.8 Hz, 1H, H3′), 6.61 (dt, J_1 = 7.6, J_2 = 0.8 Hz, 1H, H5′), 6.47 (dd, J_1 = 7.6, J_2 = 1.2 Hz, 1H, H6′), 5.05 (s, 2H, CH_2), and 3.65 (s, 3H, OMe). ^{13}C NMR (100 MHz, DMSO-d_6): δ/ppm 161.7 (CO), 157.2 (C2″), 154.9 (C2′), 148.7 (C2), 144.0 (C4), 132.4 (C4″), 131.8 (C6″), 129.2 (C4′), 128.0 (C6′), 121.1 (C1′), 120.6 (C5″), 118.8 (C5′), 117.4 (C1″), 114.9 (C3′), 111.6 (C3″), 111.0 (CN), 107.2 (C5), 55.5 (OMe), and 45.9 (CH_2). IR (nujol) $\overline{\nu}$/cm^{-1}: 3448 (m), 3332 (m), 2231 (m, CN), 1684 (m), 1668 (s, CO), and 1597 (s). Elemental analysis calcd for $C_{19}H_{16}N_4O_3$: C, 65.51; H, 4.63; N, 16.08. Found: C, 65.90; H, 4.82; N, 16.32.

*5-Cyano-1-(2-hydroxybenzyl)-2-(3-nitrophenyl)-1H-imidazole-4-carboxamide (**7l**).* Gray solid (89%). mp >300 °C. ^{1}H NMR (400 MHz, DMSO-d_6): δ/ppm 9.86 (s, 1H, OH), 7.88 (s, 1H, CONHH), 7.68 (s, 1H, CONHH), 8.43 (d, J = 2.0 Hz; 1H, H2″), 8.36 (dd, J_1 = 8.0, J_2 = 0.8 Hz; 1H, H4″), 8.05 (dd, J_1 = 8.0, J_2 = 0.8 Hz, 1H, H6″), 7.79 (t, J = 8.0 Hz; 1H, H5″), 7.10 (dt, J_1 = 8.0, J_2 = 1.6 Hz, 1H, H4′), 6.74 (d, J = 7.6 Hz, 1H, H3′), 6.73 (d, J = 7.6 Hz, 1H, H6′), 6.68 (dd, J_1 = 7.6, J_2 = 0.8 Hz, 1H, H5′), and 5.33 (s, 2H, CH_2). ^{13}C NMR (100 MHz, DMSO-d_6): δ/ppm 161.3 (CO), 154.8 (C2′),

https://doi.org/10.1021/acsomega.2c01399
ACS Omega 2022, 7, 23289−23301

148.1 (C2), 144.0 (C4), 147.7 (C3″), 135.2 (C6″), 130.4 (C5″), 130.1 (C1″), 129.5 (C4′), 128.2 (C6′), 124.8 (C4″), 123.8 (C2″), 120.7 (C1′), 119.0 (C5′), 115.2 (C3′), 110.7 (CN), 108.4 (C5), and 46.6 (CH_2). IR (nujol) $\overline{\nu}$/cm^{-1}: 3400 (m), 3352 (w), 3177 (m), 2228 (m, CN), 1685 (s, CO), and 1604 (s).

*2-(Benzo[d][1,3]dioxol-5-yl)-5-cyano-1-(2-hydroxybenzyl)-1H-imidazole-4-carboxamide (**7m**).* Light-brown solid (28%). mp 212−214 °C. ^{1}H NMR (400 MHz, DMSO-d_6): δ/ppm 9.94 (s, 1H, OH), 7.78 (s, 1H, CONHH), 7.63 (s, 1H, CONHH), 7.13 (d, J = 1.6 Hz, 1H, H2″), 7.10 (t, J = 8 Hz, 1H, H4′), 7.09 (dd, J_1 = 8.0, J_2 = 1.6 Hz, 1H, H6″), 7.02 (d, J = 8 Hz, 1H, H5″), 6.81 (d, J = 8 Hz, 1H, H3′), 6.72 (t, J = 7.6 Hz, 1H, H5′), 6.56 (d, J = 6.8 Hz, 1H, H6′), 6.08 (s, 2H, OCH_2O), and 5.28 (s, 2H, CH_2). ^{13}C NMR (100 MHz, DMSO-d_6): δ/ppm 161.6 (CO), 154.5 (C2′), 150.2 (C2), 148.9 (C3″), 147.5 (C4″), 143.9 (C4), 129.3 (C4′), 127.0 (C6′), 123.4 (C6″), 121.9 (C1″), 121.3 (C1′), 119.2 (C5′), 115.2 (C3′), 109.0 (C2″), 108.7 (C5″), 107.5 (C5), 101.8 (Ca), and 46.2 (CH_2). IR (nujol) $\overline{\nu}$/cm^{-1}: 3581 (m), 3482 (w), 3433 (m), 3351 (w), 3187 (m), 2227 (s, CN), 1688 (s, CO), and 1603 (s). Elemental analysis calcd for $C_{19}H_{14}N_4O_4$·H_2O: C, 61.03; H, 4.12; N, 14.99. Found: C, 60.73; H, 4.43; N, 14.76.

*5-Cyano-1-(2-hydroxybenzyl)-2-(6-methoxynaphthalen-2-yl)-1H-imidazole-4-carboxamide (**7n**).* Light-purple solid (54%). mp 142−144 °C. ^{1}H NMR (400 MHz, DMSO-d_6): δ/ppm 10.06 (s, 1H, OH), 7.83 (s, 1H, CONHH), 7.63 (s, 1H, CONHH), 8.09 (d, J = 1.2 Hz, 1H, H1″), 7.89 (d, J = 8.8 Hz, 1H, H8″), 7.80 (d, J = 9.2 Hz, 1H, H4″), 7.68 (dd, J_1 = 8.4, J_2 = 1.6 Hz, 1H, H3″), 7.37 (d, J = 2.4 Hz, 1H, H5″), 7.22 (dd, J_1 = 9.2, J_2 = 2.4 Hz, 1H, H7″), 7.10 (dt, J_1 = 8.0, J_2 = 2.0 Hz, 1H, H4′), 6.80 (dd, J_1 = 8.0, J_2 = 1.6 Hz, 1H, H3′), 6.68 (dt, J_1 = 8.0, J_2 = 0.8 Hz, 1H, H5′), 6.62 (dd, J_1 = 7.6, J_2 = 0.8 Hz, 1H, H6′), 5.39 (s, 2H, CH_2), and 3.92 (s, 3H, OMe). ^{13}C NMR (100 MHz, DMSO-d_6): δ/ppm 161.3 (CO), 158.5 (C6″), 154.6 (C2′), 150.7 (C2), 144.1 (C4), 134.8 (C2″), 130.0 (C4″), 129.3 (C4′), 128.6 (C1″), 127.6 (C10″), 127.2 (C6′ and C8″), 126.2 (C3″), 123.4 (C9″), 119.7 (C7″), 119.1 (C5′), 115.1 (C3′), 111.0 (CN), 107.8 (C5), 106.0 (C5″), 55.4 (OMe), and 46.2 (CH_2). IR (nujol) $\overline{\nu}$/cm^{-1}: 3466 (s), 3477 (w), 3278 (w), 3169 (m), 2226 (m, CN), 1683 (s, CO), 1628 (s) and 1603 (s). Elemental analysis calcd for $C_{23}H_{18}N_4O_3$·0.25H_2O: C, 68.72; H, 4.61; N, 13.94. Found: C, 68.78; H, 5.23; N, 13.69.

*5-Cyano-2-(furan-2-yl)-1-(2-hydroxybenzyl)-1H-imidazole-4-carboxamide (**7o**).* Light-brown solid (53%). mp 227−229 °C. ^{1}H NMR (400 MHz, DMSO-d_6): δ/ppm 9.99 (s, 1H, OH), 7.89 (d, J = 1.2 Hz, 1H, H4″), 7.78 (s, 1H, CONHH), 7.69 (s, 1H, CONHH), 7.12 (dt, J_1 = 7.2, J_2 = 1.2 Hz, 1H, H4′), 6.95 (dd, J_1 = 7.6, J_2 = 0.4 Hz, 1H, H2″), 6.83 (dd, J_1 = 8.0, J_2 = 0.4 Hz, 1H, H3′), 6.71 (dt, J_1 = 7.6, J_2 = 0.8 Hz, 1H, H5′), 6.67 (dd, J_1 = 3.6, J_2 = 1.6 Hz, 1H, H3″), 6.59 (dd, J_1 = 7.6, J_2 = 1.2 Hz, 1H, H6′), and 5.48 (s, 2H, CH_2). ^{13}C NMR (100 MHz, DMSO-d_6): δ/ppm 161.3 (CO), 154.7 (C2′), 145.3 (C3″), 144.2 (C4), 142.7 (C1″), 141.3 (C2), 129.2 (C4′), 126.9 (C6′), 121.2 (C1′), 119.1 (C5′), 115.2 (C3′), 113.1 (C5″), 112.1 (C4″), 110.7 (CN), 107.8 (C5), and 46.2 (CH_2). IR (nujol) $\overline{\nu}$/cm^{-1}: 3445 (m), 3335 (m), 2234 (m, CN), 1675 (s, CO), 1659 (s) and 1596 (s). Elemental analysis calcd for $C_{16}H_{12}N_4O_3$: C, 62.33; H, 3.92; N, 18.17. Found: C, 62.56; H, 3.91; N, 18.25.

*5-Cyano-1-(2-hydroxy-3-methoxybenzyl)-2-(3-nitrophenyl)-1H-imidazole-4-carboxamide (**7p**).* Beige solid (49%). mp 203−205 °C. ^{1}H NMR (400 MHz, DMSO-d_6): δ/ppm 9.09 (s, 1H, OH), 7.89 (s, 1H, CONHH), 7.68 (s, 1H, CONHH), 8.40 (t, J = 1.6 Hz, 1H, H2″), 8.33 (ddd, J_1 = 7.6, J_2 = 2.4, J_3 = 0.8 Hz, 1H, H4″), 8.04 (d, J = 8.0 Hz, 1H, H6″), 7.78 (t, J = 8.0 Hz, 1H, H5″), 6.90 (dd, J_1 = 8.0, J_2 = 0.8 Hz, 1H, H4′), 6.69 (t, J = 8.0 Hz, 1H, H5′), 6.35 (dd, J_1 = 7.6, J_2 = 0.8 Hz, 1H, H6′), 5.35 (s, 2H, CH_2), and 3.75 (s, 3H, OMe). ^{13}C NMR (100 MHz, DMSO-d_6): δ/ppm 161.4 (CO), 147.8 (C3″), 147.5 (C3′), 143.5 (C2′), 148.3 (C2), 144.1 (C4), 135.1 (C6″), 130.4 (C5″), 130.0 (C1″), 124.8 (C4″), 124.0 (C2″), 121.3 (C1′), 119.9 (C6′), 119.0 (C5′), 111.9 (C4′), 110.7 (CN), 108.3 (C5), 55.8 (OMe), and 46.5 (CH_2). IR (nujol) $\overline{\nu}$/cm^{-1}: 3483 (s), 3448 (m), 3375 (s), 3294 (m), 2226 (m, CN), 1683 (s), 1674 (s, CO), and 1593 (s). Elemental analysis calcd for $C_{19}H_{15}N_5O_5$: C, 58.01; H, 3.84; N, 17.80. Found: C, 58.24; H, 3.92; N, 17.72.

*2-(2-Chlorophenyl)-5-cyano-1-(2-hydroxy-3-methoxybenzyl)-1H-imidazole-4-carboxamide (**7q**).* Beige solid (51%). mp 260−262 °C. ^{1}H NMR (400 MHz, DMSO-d_6): δ/ppm 9.01 (s, 1H, OH), 7.81 (s, 1H, CONHH), 7.63 (s, 1H, CONHH), 7.55 (dt, J_1 = 8.0, J_2 = 1.6 Hz, 1H, H4″), 7.54 (dd, J_1 = 8.0, J_2 = 1.6 Hz, 1H, H3″), 7.43 (dd, J_1 = 7.2, J_2 = 1.6 Hz, 1H, H6″), 7.42 (dt, J_1 = 7.6, J_2 = 1.6 Hz, 1H, H5″), 6.85 (dd, J_1 = 8.0, J_2 = 1.6 Hz, 1H, H4′), 6.59 (t, J = 8.0 Hz, 1H, H5′), 6.12 (dd, J_1 = 7.6, J_2 = 1.2 Hz, 1H, H6′), 5.10 (s, 2H, CH_2), and 3.73 (s, 3H, OMe). ^{13}C NMR (100 MHz, DMSO-d_6): δ/ppm 161.4 (CO), 147.7 (C2), 147.3 (C3′), 144.0 (C2′), 143.7 (C4), 133.3 (C1″), 132.4 (C4″), 132.3 (C6″), 129.5 (C3″), 127.7 (C2″), 127.3 (C5″), 120.9 (C1′), 119.7 (C6′), 118.6 (C5′), 111.9 (C4′), 110.6 (CN), 107.3 (C5), 55.8 (OMe), and 45.9 (CH_2). IR (nujol) $\overline{\nu}$/cm^{-1}: 3487 (m), 3373 (m), 2232 (m, CN), 1677 (s, CO), and 1592 (s). Elemental analysis calcd for $C_{19}H_{15}ClN_4O_3$: C, 59.61; H, 3.95; N, 14.64. Found: C, 59.98; H, 4.11; N, 14.93.

*2-(2-Bromophenyl)-5-cyano-1-((2-hydroxynaphthalen-1-yl)methyl)-1H-imidazole-4-carboxamide (**7r**).* Pale brown solid (73%). mp 231−233 °C. ^{1}H NMR (500 MHz, DMSO-d_6): δ/ppm 10.21 (s, 1H, OH), 7.75 (s, 1H, CONHH), 7.71 (t, J = 8.9 Hz, 1H, H4′), 7.70 (d, J = 7.5 Hz, 1H, H6″), 7.56 (s, 1H, CONHH), 7.49 (t, J = 7.3 Hz, 1H, H5″), 7.43 (d, J = 7.6 Hz, 1H, H8′), 7.25 (t, J = 7.6 Hz, 1H, H7′), 7.21 (m, 4H, H6′ + H5′ + H4″ + H3″), 7.04 (d, J = 8.8 Hz, 1H, H3′), and 5.58 (s, 2H, CH_2). ^{13}C NMR (125 MHz, DMSO-d_6): δ/ppm 161.5 (CO), 155.0 (C2′), 148.6 (C2), 143.0 (C4), 132.4 (C5″), 132.2 (C4″), 131.9 (C3″), 131.7 (C4′), 130.7 (C1″), 130.0 (C8a′), 128.2 (C6″), 127.4 (C5′), 127.2 (C2″), 126.6 (C7′), 123.4 (C4a′), 122.2 (C6′), 120.8 (C8′), 117.5 (C3′), 110.6 (C1′), 110.5 (CN), 107.7 (C5), and 42.1 (CH_2). IR (ATR) $\overline{\nu}$/cm^{-1}: 3350 (m), 2232 (m, CN), 1668 (s, CO), 1598 (m), 1447 (m), and 1019 (m). MS (ESI) m/z: 447 and 449 (MH^+). HRMS calcd for $C_{22}H_{16}{}^{79}BrN_4O_2$ (MH^+): 447.0449; found, 447.0451.

*6-(2-Chlorophenyl)-3-cyano-5-(3-hydroxyphenyl)-1,6-dihydropyrazine-2-carboxamide (**10**).* A solution of imine **8** (0.2 g, 0.94 mmol) in ethanol (2 mL) at room temperature was treated with 2-chlorobenzaldehyde (127 μL, 1.13 mmol) and Et_3N (1.88 mmol, 262 μL), and the reaction mixture was stirred for 96 h. The resulting yellow solid was filtered and successively washed with cold ethanol, methanol, and diethyl ether. A sample (9 mg) of the solid was solubilized in DMSO-d_6 (250 μL), and the mixture was heated at 80 °C for 30 min.

https://doi.org/10.1021/acsomega.2c01399
ACS Omega 2022, 7, 23289−23301

After this time, the mixture was studied by ^{1}H and ^{13}C NMR spectroscopy, with dihydropyrazine **10** being identified. ^{1}H NMR (400 MHz, DMSO-d_6): δ/ppm 9.62 (s, 1H, OH), 8.66 (d, J = 2.8 Hz, 1H, NH), 8.06 (s, 1H, CONH*H*), 7.94 (s, 1H, CONH*H*), 7.55 (dd, J_1 = 7.6 Hz, J_2 = 1.2 Hz, 1H, H3″), 7.37 (dt, J_1 = 7.6 Hz, J_2 = 1.6 Hz, 1H, H4″), 7.31 (dt, J_1 = 7.6, J_2 = 1.6 Hz, 1H, H5″), 7.22 (t, J = 2.0 Hz, 1H, H2′), 7.18 (t, J = 8.0 Hz, 1H, H5′), 7.07 (dd, J_1 = 7.6, J_2 = 1.6 Hz, 2H, H6′ + H6″), 6.78 (dd, J_1 = 8.0, J_2 = 2.5 Hz, 1H, H4′), and 6.16 (d, J = 2.8 Hz, 1H, CH). ^{13}C NMR (100 MHz, DMSO-d_6): δ/ppm 162.3 (CO), 157.6 (C3′), 145.2 (C5), 140.6 (C2), 136.1 (C1′), 135.4 (C1″), 131.4 (C2″), 130.6 (C4″), 130.3 (C3″), 129.8 (C5′), 129.4 (C6″), 119.1 (CN), 117.8 (C4′), 117.1 (C6′), 112.9 (C2′), 96.2 (C3), and 48.6 (C6). IR (nujol) $\overline{\nu}$/cm^{-1}: 3475 (w), 3270 (m), 2205 (s, CN), 1672 (s, CO), 1558 (m), and 1533 (m).

Computational Studies. All calculations were initially performed in vacuum using the program Gaussian 09[27] at the B3LYP level of theory and the basis set TZVP.[29] Transition states and intermediates were further refined considering Grimme's correction[28] and the solvent effect (CPCM,[26] ethanol). The imaginary frequencies calculated for all the transition states identified in the reaction path are summarized in Table S1.

Step 1—intramolecular cyclization: to find a starting point for determining the transition states of the two possible cyclization reactions [formation of the five-membered compounds (path a) and six-membered heterocycles (path b)], a relaxed potential energy surface (PES) was calculated for the three possible isomers (*ortho*, *meta*, and *para*) of each path, and the two possible protonation forms of the phenol group were explored (neutral and phenoxide). No substituent (aryl) was considered in the whole calculation. The two possible relative arrangements of the substituents −CN and −CONH$_2$ were considered, that is, with either the NH$_2$ group or the carbonyl group in the CONH$_2$ moiety pointing toward the CN substituent. To identify the transition state, an elongation of the bond formed in the reaction from 1.6 to 2.5 Å was applied by always taking the last step of the previous distance as the starting point of the next one. For the formation of five-membered structures, the distance between the nitrogen atom connected to the benzyl group (N1) and the methylenic carbon atom (Cb) was considered. For the formation of six-membered structures, the distance between the benzylenic carbon atom (Ca) and Cb was used. The highest energy points of these PES calculations were then used as the starting point for the identification of the transition states. Finally, to obtain both the starting and end points of the reaction, an IRC approach was performed in both the forward and reverse directions. In all cases, the final step of the IRC calculation was further minimized to obtain a local minimum for each structure.

Step 2—aromatization: a similar protocol to that described for step 1 (phenoxide form) was employed here but considering a two-stage process: (i) abstraction of the hydrogen atom in the previously obtained nitrogen heterocycle by the phenoxide group and (ii) transfer of the hydrogen atom from the resulting phenol group to the benzylidene carbon atom (Ca). For both stages, the elongation was performed from 1.3 to 3.0 Å, starting from the previously obtained intermediate **B.O** in the case of stage i and from the resulting intermediate of the latter (intermediate **INT**) in the case of stage ii. All the identified transition states were characterized by having an imaginary frequency that corresponds to the formation of the O−H bond (**TS3** and **TS3_Ph**) or of the Cα−H bond (**TS4** and **TS4_Ph**) (Table S1). Cartesian coordinates (PDB1−24), total electronic energies, and thermal corrections (Table S2) are included in the Supporting Information.

■ ASSOCIATED CONTENT

Supporting Information

The Supporting Information is available free of charge at https://pubs.acs.org/doi/10.1021/acsomega.2c01399.

Free energy profiles for the cyclization steps involving compounds **A.OH** and **A.O** to afford five- and six-membered derivatives substituted with 2-, 3-, and 4-phenol groups; imaginary frequencies calculated for the transition states identified in the reaction path; geometries of the transition states obtained by computational studies; total electronic energies and thermal corrections; geometries of the intermediates obtained by computational studies; free energy profiles for the cyclization steps involving compounds **A.OH_Ph** and **A.O_Ph** to afford five- and six-membered derivatives substituted with 2-, 3-, and 4-phenol groups; and NMR spectra of compounds **7**, **10**, and **6c** (PDF)

Cartesian coordinates of **TS1.OH** (PDB1) (PDB)

Cartesian coordinates of **TS1.O** (PDB2) (PDB)

Cartesian coordinates of **TS1.OH_Ph** (PDB3) (PDB)

Cartesian coordinates of **TS1.O_Ph** (PDB4) (PDB)

Cartesian coordinates of **TS2.OH** (PDB5) (PDB)

Cartesian coordinates of **TS2.O** (PDB6) (PDB)

Cartesian coordinates of **TS2.OH_Ph** (PDB7) (PDB)

Cartesian coordinates of **TS2.O_Ph** (PDB8) (PDB)

Cartesian coordinates of **TS3** (PDB9) (PDB)

Cartesian coordinates of **TS3_Ph** (PDB10) (PDB)

Cartesian coordinates of **INT** (PDB11) (PDB)

Cartesian coordinates of **INT_Ph** (PDB12) (PDB)

Cartesian coordinates of **TS4** (PDB13) (PDB)

Cartesian coordinates of **TS4_Ph** (PDB14) (PDB)

Cartesian coordinates of **B.OH** (PDB15) (PDB)

Cartesian coordinates of **B.O** (PDB16) (PDB)

Cartesian coordinates of **B.OH_Ph** (PDB17) (PDB)

Cartesian coordinates of **B.O_Ph** (PDB18) (PDB)

Cartesian coordinates of **C.OH** (PDB19) (PDB)

Cartesian coordinates of **C.O** (PDB20) (PDB)

Cartesian coordinates of **C.OH_Ph** (PDB21) (PDB)

Cartesian coordinates of **C.O_Ph** (PDB22) (PDB)

Cartesian coordinates of **D.O** (PDB23) (PDB)

Cartesian coordinates of **D.O_Ph** (PDB24) (PDB)

■ AUTHOR INFORMATION

Corresponding Authors

Concepción González-Bello − *Centro Singular de Investigación en Química Biolóxica e Materiais Moleculares (CiQUS), Departamento de Química Orgánica, Universidade de Santiago de Compostela, 15782 Santiago de Compostela, Spain;* orcid.org/0000-0001-6439-553X; Email: concepcion.gonzalez.bello@usc.es

M. Fernanda Proença − *Department of Chemistry, University of Minho, 4710-057 Braga, Portugal*; Email: fproenca@quimica.uminho.pt

https://doi.org/10.1021/acsomega.2c01399
ACS Omega 2022, 7, 23289−23301

Authors

Fábio Pedroso de Lima − *Department of Chemistry, University of Minho, 4710-057 Braga, Portugal*

Emilio Lence − *Centro Singular de Investigación en Química Biolóxica e Materiais Moleculares (CiQUS), Departamento de Química Orgánica, Universidade de Santiago de Compostela, 15782 Santiago de Compostela, Spain*

Pilar Suárez de Cepeda − *Centro Singular de Investigación en Química Biolóxica e Materiais Moleculares (CiQUS), Departamento de Química Orgánica, Universidade de Santiago de Compostela, 15782 Santiago de Compostela, Spain*

Carla Correia − *Department of Chemistry, University of Minho, 4710-057 Braga, Portugal*

M. Alice Carvalho − *Department of Chemistry, University of Minho, 4710-057 Braga, Portugal*

Complete contact information is available at: https://pubs.acs.org/10.1021/acsomega.2c01399

Author Contributions

[§]F.P.d.L. and E.L. contributed equally to this work.

Notes

The authors declare no competing financial interest.

■ ACKNOWLEDGMENTS

Financial support from Axencia Galega de Innovación (2020-PG067, CG-B), Programa NORTE 2020—CCDR-N (ref. NORTE-08-5369-FSE-000033, MFP), the Spanish Ministry of Science and Innovation (PID2019-105512RB-I00, CG-B), the Xunta de Galicia [ED431C 2021/29 and the Centro singular de investigación de Galicia accreditation 2019−2022 (ED431G 2019/03), CG-B], and the European Regional Development Fund (ERDF) is gratefully acknowledged. All authors thank the Centro de Supercomputación de Galicia (CESGA) for the use of the Finis Terrae computer.

■ REFERENCES

(1) Al-Azmi, A.; Elassar, A.-Z. A.; Booth, B. L. The chemistry of diaminomaleonitrile and its utility in heterocyclic synthesis. *Tetrahedron* **2003**, *59*, 2749−2763.

(2) Ohtsuka, Y. Chemistry of diaminomaleonitrile. 3. Reaction with isocyanate: a novel pyrimidine synthesis. *J. Org. Chem.* **1978**, *43*, 3231−3234.

(3) Ohtsuka, Y. Chemistry of diaminomaleonitrile. 4. Nitrile hydration of the Schiff bases. *J. Org. Chem.* **1979**, *44*, 827−830.

(4) Shirai, K.; Matsuoka, M.; Fukunishi, K. New syntheses and solid state fluorescence of azomethine dyes derived from diaminomaleonitrile and 2,5-diamino-3,6-dicyanopyrazine. *Dyes Pigm.* **2000**, *47*, 107−115.

(5) Booth, B. L.; Dias, A. M.; Proença, M. F.; Zaki, M. E. A. The reactions of diaminomaleonitrile with isocyanates and either aldehydes or ketones revisited. *J. Org. Chem.* **2001**, *66*, 8436−8441.

(6) Alves, M. J.; Booth, B. L.; Proenç, M. F. J. R. P. Synthesis of 5-amino-4-(cyanoformimidoyl)-1H-imidazole: a reactive intermediate for the synthesis of 6-carbamoyl-1,2-dihydropurines and 6-carbamoylpurines. *J. Chem. Soc., Perkin Trans. 2* **1990**, 1705−1712.

(7) Carvalho, M. A.; Esperança, S.; Esteves, T.; Proença, M. F. An Efficient synthesis of 7,8-dihydropyrimido[5,4-d]pyrimidines. *Eur. J. Org. Chem.* **2007**, 1324−1331.

(8) Sun, Z.; Hosmane, R. S. An improved synthesis of 9-benzyladenine: a model for adenosine and its analogues. *Synth. Commun.* **2001**, *31*, 549−554.

(9) Bettencourt, A.; Castro, M.; Silva, J.; Fernandes, F.; Coutinho, O.; Sousa, M.; Proença, M.; Areias, F. New nitrogen compounds coupled to phenolic units with antioxidant and antifungal activities: synthesis and structure−activity relationship. *Molecules* **2018**, *23*, 2530.

(10) Zheng, K.; Chen, H.; Xiao, Y.; Yan, J.; Zhang, N.; Liu, X. CuO_x/OMS-2 catalyzed synthesis of 4,5-dicyano-1*H*-imidazoles moiety: directly access to D-A system for AIE-active mechanofluorochromic materials. *J. Mol. Struct.* **2022**, *1250*, 131791.

(11) Alves, M. J.; Carvalho, M. A.; Proença, M. F. J. R. P.; Booth, B. L.; Pritchard, R. G. Synthesis of 6-cyanopurines and the isolation and X-ray structure of novel 2*H*-pyrroles. *J. Heterocycl. Chem.* **1997**, *34*, 739−743.

(12) Alves, M. J.; Carvalho, M. A.; Fernanda, M.; Proença, J. R. P.; Booth, B. L.; Pritchard, R. G. Synthesis and mechanism of formation of novel 2,5-dihydro-2,5-diimino-3,4-di[(N,N-dimethylamino)-methylideneamino]pyrroles and 5-amino-3,4-di[(N,N-dimethylamino)methylideneamino]-2*H*-2-iminopyrroles. *J. Heterocycl. Chem.* **1999**, *36*, 193−199.

(13) Rivera, A.; Ríos-Motta, J. R.-M.; León, F. Revisiting the reaction between diaminomaleonitrile and aromatic aldehydes: a green chemistry approach. *Molecules* **2006**, *11*, 858−866.

(14) Rulhania, S.; Kumar, S.; Nehra, B.; Gupta, G.; Monga, V. An insight into the medicinal perspective of synthetic analogs of imidazole. *J. Mol. Struct.* **2021**, *1232*, 129982.

(15) Siwach, A.; Verma, P. K. Synthesis and therapeutic potential of imidazole containing compounds. *BMC Chem.* **2021**, *15*, 12.

(16) Andrei, G. S.; Andrei, B. F.; Roxana, P. R. Imidazole derivatives and their antibacterial activity - a mini-review. *Mini-Rev. Med. Chem.* **2021**, *21*, 1380−1392.

(17) Parwani, D.; Bhattacharya, S.; Rathore, A.; Mallick, C.; Asati, V.; Agarwal, S.; Rajoriya, V.; Das, R.; Kashaw, S. K.; Sushil, K. Current insights into the chemistry and antitubercular potential of benzimidazole and imidazole derivatives. *Mini-Rev. Med. Chem.* **2021**, *21*, 643−657.

(18) Ribeiro, A. I.; Gabriel, C.; Cerqueira, F.; Maia, M.; Pinto, E.; Sousa, J. C.; Medeiros, R.; Proença, M. F.; Dias, A. M. Synthesis and antimicrobial activity of novel 5-aminoimidazole-4-carboxamidrazone. *Bioorg. Med. Chem. Lett.* **2014**, *24*, 4699−4702.

(19) Sharma, P.; LaRosa, C.; Antwi, J.; Govindarajan, R.; Werbovetz, K. A. Imidazoles as potential anticancer agents: an update on recent studies. *Molecules* **2021**, *26*, 4213.

(20) Ali, I.; Lone, M. N.; Aboul-Enein, H. Y.; Haasan, Y. Imidazoles as potential anticancer agents. *MedChemComm* **2017**, *8*, 1742−1773.

(21) Dolezal, M.; Zitko, J. Quinazoline derivatives as anticancer drugs: a patent review (2011 - present). *Expert Opin. Ther. Pat.* **2015**, *25*, 33−47.

(22) Sreekanth Reddy, O.; Lai, W. F. Tackling COVID-19 using remdesivir and favipiravir as therapeutic options. *ChemBioChem* **2021**, *22*, 939−948.

(23) Miniyar, P.; Murumkar, P.; Patil, P.; Barmade, M.; Bothara, K. Unequivocal role of pyrazine ring in medicinally important compounds: a review. *Mini-Rev. Med. Chem.* **2013**, *13*, 1607−1625.

(24) Potter, A.; Oldfield, V.; Nunns, C.; Fromont, C.; Ray, S.; Northfield, C. J.; Bryant, C. J.; Scrace, S. F.; Robinson, D.; Matossova, N.; Baker, L.; Dokurno, P.; Surgenor, A. E.; Davis, B.; Richardson, C. M.; Murray, J. B.; Moore, J. D. Discovery of cell-active phenyl-imidazole Pin1 inhibitors by structure-guided fragment evolution. *Bioorg. Med. Chem. Lett.* **2010**, *20*, 6483.

(25) Ohtsuka, Y.; Tohma, E.; Kojima, S.; Tomita, N. Chemistry of diaminomaleonitrile. 5. Dihydropyrazine synthesis. *J. Org. Chem.* **1979**, *44*, 4871−4876.

(26) Barone, V.; Cossi, M. Quantum calculation of molecular energies and energy gradients in solution by a conductor solvent model. *J. Phys. Chem. A* **1998**, *102*, 1995−2001.

(27) Frisch, M. J.; Trucks, G. W.; Schlegel, H. B.; Scuseria, G. E.; Robb, M. A.; Cheeseman, J. R.; Scalmani, G.; Barone, V.; Mennucci, B.; Petersson, G. A.; Nakatsuji, H.; Caricato, M.; Li, X.; Hratchian, H. P.; Izmaylov, A. F.; Bloino, J.; Zheng, G.; Sonnenberg, J. L.; Hada, M.; Ehara, M.; Toyota, K.; Fukuda, R.; Hasegawa, J.; Ishida, M.; Nakajima, T.; Honda, Y.; Kitao, O.; Nakai, H.; Vreven, T.; Montgomery, J. A.; Peralta, J. E.; Ogliaro, F.; Bearpark, M.; Heyd,

J. J.; Brothers, E.; Kudin, K. N.; Staroverov, V. N.; Kobayashi, R.; Normand, J.; Raghavachari, K.; Rendell, A.; Burant, J. C.; Iyengar, S. S.; Tomasi, J.; Cossi, M.; Rega, N.; Millam, J. M.; Klene, M.; Knox, J. E.; Cross, J. B.; Bakken, V.; Adamo, C.; Jaramillo, J.; Gomperts, R.; Stratmann, R. E.; Yazyev, O.; Austin, A. J.; Cammi, R.; Pomelli, C.; Ochterski, J. W.; Martin, R. L.; Morokuma, K.; Zakrzewski, V. G.; Voth, G. A.; Salvador, P.; Dannenberg, J. J.; Dapprich, S.; Daniels, A. D.; Farkas, Ö.; Foresman, J. B.; Ortiz, J. V.; Cioslowski, J.; Fox, D. J. *Gaussian 09*, Revision D.01; Gaussian, Inc.: Wallingford CT, 2009.

(28) Grimme, S. Density functional theory with London dispersion corrections. *Wiley Interdiscip. Rev.: Comput. Mol. Sci.* **2011**, *1*, 211−228.

(29) Boys, S. F.; Bernardi, F. The calculation of small molecular interactions by the differences of separate total energies. Some procedures with reduced errors. *Mol. Phys.* **1970**, *19*, 553−566.

https://doi.org/10.1021/acsomega.2c01399
ACS Omega 2022, 7, 23289−23301